

Fast Neural Architecture Search of Compact Semantic Segmentation Models via Auxiliary Cells*

Vladimir Nekrasov[†] Hao Chen[†] Chunhua Shen Ian Reid
The University of Adelaide, Australia

E-mail: {vladimir.nekrasov, hao.chen01, chunhua.shen, ian.reid}@adelaide.edu.au

Abstract

Automated design of architectures tailored for a specific task at hand is an extremely promising, albeit inherently difficult, venue to explore. While most results in this domain have been achieved on image classification and language modelling problems, here we concentrate on dense per-pixel tasks, in particular, semantic image segmentation using fully convolutional networks. In contrast to the aforementioned areas, the design choice of a fully convolutional network requires several changes, ranging from the sort of operations that need to be used—e.g., dilated convolutions—to solving of a more difficult optimisation problem.

In this work, we are particularly interested in searching for high-performance compact segmentation architectures, able to run in real-time using limited resources. To achieve that, we intentionally over-parameterise the architecture during the training time via a set of auxiliary cells that provide an intermediate supervisory signal and can be omitted during the evaluation phase. The design of the auxiliary cell is emitted by a controller, a neural architecture with the fixed structure trained using reinforcement learning. More crucially, we demonstrate how to efficiently search for these architectures within limited time and computational budgets. In particular, we rely on a progressive strategy that terminates non-promising architectures from being further trained, and on Polyak averaging coupled with knowledge distillation to speed-up the convergence. Quantitatively, in 8 GPU-days our approach discovers a set of architectures performing on-par with state-of-the-art among compact models.

1. Introduction

For years, the design of neural network architectures was thought to be solely a duty of a human expert - it was her responsibility to specify which type of architecture to

use, how many layers should there be, how many channels should convolutional layers have and etc. This is no longer the case as the automated neural architecture search - a way of predicting the neural network structure via a non-human expert (an algorithm) - is becoming prevalent. Potentially, this may well mean that instead of manually adapting a single state-of-the-art architecture for a new task at hand, the algorithm would discover a set of best-suited and high-performing architectures on given data.

Few decades ago, such an algorithm was based on evolutionary programming strategies where best seen so far architectures underwent mutations and their most promising off-springs were bound to continue evolving [2]. Now, we have reached the stage where a secondary neural network, oftentimes called *controller*, replaces a human in the loop, by iteratively searching among possible architecture candidates and maximising the expected score on the held-out set [46]. While there is a lack of theoretical work behind this latter approach, several promising empirical breakthroughs have already been achieved [3, 47].

At this point, it is important to emphasise the fact that such accomplishments required an excessive amount of computational resources—more than 20,000 GPU-days for the work of Zoph and Le [46] and 2,000 for Zoph *et al.* [47]. While few works have reduced those to single digit numbers on image classification and language processing tasks [21, 28], we consider more challenging dense per-pixel tasks that produce an output for each pixel in the input image. Although here we concentrate only on semantic image segmentation, our proposed methodology can immediately be applied to other per-pixel prediction tasks, such as depth estimation and surface normal estimation. Notably, all of them play an important role in computer vision and robotic applications, relying on manually designed accurate low-latency models for real-world scenarios.

The focus of our work is to automatically discover compact high-performing fully convolutional architectures, able to run in real-time on a low-computational budget, for example, on the Jetson platform. To this end, we are explicitly looking for structures that not only improve the perfor-

*Preprint. Work in Progress.

[†]Equal contribution.

mance on the held-out set, but also facilitate the optimisation during the training stage. Concretely, we consider the encoder-decoder type of a fully-convolutional network [23], where encoder is represented by a pre-trained image classifier, and the decoder structure is emitted by the controller network. The controller generates the connectivity structure between encoder and decoder, as well as the sequence of operations (that form the so-called *cell*) to be applied on each connected path. The same cell structure is used to form an auxiliary classifier, the goal of which is to provide intermediate supervision and to implicitly over-parameterise the model. Over-parameterisation is believed to be the primary reason behind the successes of deep learning models, and few theoretical works have already addressed it in simplified cases [8, 37]. Along with empirical results, this is the primary motivation behind the described approach.

Last, but not the least, we devise a search strategy that permits to find high-performing architectures within a small number of days using only few GPUs. Concretely, we pursue two goals here:

- i.) To prevent ‘bad’ architectures from being trained for long; and
- ii.) To achieve a solid performance estimate as soon as possible.

To tackle the first goal, we divide the training process during the search into two stages. During the first stage, we fix the encoder’s weights and pre-compute its outputs, while only training the decoder part. For the second stage, we train the whole model end-to-end. We validate the performance after the first stage and terminate the training of non-promising architectures. For the second goal, we employ Polyak averaging [29] and knowledge distillation [13] to speed-up convergence.

To summarise, our contributions in this work are to propose an efficient neural architecture search strategy for dense-per-pixel tasks that (i.) allows to sample compact high-performing architectures, and (ii.) can be used in real-time on low-computing platforms, such as JetsonTX2. In particular, the above points are made possible by:

- Devising a progressive strategy able to eliminate poor candidates early in the training;
- Developing a training schedule for semantic segmentation able to provide solid results quickly via the means of knowledge distillation and Polyak averaging;
- Searching for an over-parameterised auxiliary cell that provides better training, which is obsolete during inference.

2. Related Work

Traditionally, architecture search methods have been relying upon evolutionary strategies [2, 39, 40], where

a population of networks (oftentimes together with their weights) is continuously mutated, and less promising networks are being discarded. Modern neuro-evolutionary approaches [22, 30] rely on the same principles and benefit from available computational resources, that allow them to achieve impressive results. Bayesian optimisation methods estimating the probability density of objective function have long been used for hyper-parameter search [4, 36]. Scaling up Bayesian methods for architecture search is an ongoing work, and few kernel-based approaches have already shown solid performance [15, 41].

Most recently, neural architecture search (NAS) strategies based on reinforcement learning (RL) have attained state-of-the-art results on the tasks of image classification and natural language processing [3, 46, 47]. Relying on enormous computational resources, these algorithms comprise a separate neural network, controller, that emits an architecture design and receives a scalar reward after the emitted architecture is trained on the task of interest. Notably, to converge thousands of iterations and GPU-days are needed. Rather than searching for the whole network structure from scratch, these methods tend to look for *cells*—repeatable motifs that can be stacked multiple times in a feedforward fashion.

Several solutions for making NAS methods more efficient have been recently proposed. In particular, Pham *et al.* [28] unroll the computational graph of all possible architectures and allow to share the weights among different architectures. This dramatically reduces the number of resources needed for convergence. In a similar vein of research, Liu *et al.* [21] exploit a progressive strategy where the network complexity is gradually increased, while the ranking network is trained in parallel to predict the performance of a new architecture. Few methods have been built around the continuous relaxation of the search problem. Particularly Luo *et al.* [24] use an encoder to embed the architecture description into a latent space, and estimator to predict the performance of an architecture given its embedding. While these methods make the search process more efficient, they achieve so by sacrificing the expressiveness of the search space, and hence, may arrive to a sub-optimal solution.

In semantic segmentation [18, 19], up to now all the architectures have been manually designed, closely following the winner entries of image classification challenges. Two prominent directions have emerged over the last few years: the encoder-decoder type [18, 23, 27], where better features are learned at the expense of having a spatially coarse output mask; whereas other popular approach discards several down-sampling layers and relies on dilated convolutions for keeping the receptive field size intact [6, 43, 45]. Chen *et al.* [7] have also shown that the combination of those two paradigms lead to even better results across different bench-

marks. In terms of NAS in semantic segmentation, independently of us and in parallel to our work, a straightforward adaptation of image classification NAS methods was proposed by Chen *et al.* [5]. In it they randomly search for a single segmentation cell design and achieve expressive results by using *almost 400 GPUs over the range of 7 days*. In contrast to that, our method first and foremost is able to find compact segmentation models only in a fraction of that time. Secondly, it differs significantly in terms of the search design and search methodology.

For the purposes of a clearer presentation of our ideas, we briefly review knowledge distillation, an approach proposed by Hinton *et al.* [13] to successfully train a compact model using the outputs of a single (or an ensemble of) large network(s) pre-trained on the current task. In it, the logits of the pre-trained network are being used as an additional regulariser for the small network. In other words, the latter has to mimic the outputs of the former. Such a method was shown to provide a better learning signal for the small network. As a result of that, it has already found its way across multiple domains: computer vision [44], reinforcement learning [31], continuous learning [17], to name a few.

3. Methodology

We start with the problem formulation, proceed with the definitions of an auxiliary cell and knowledge distillation loss, and conclude with the overall search strategy.

We primarily focus on two research questions: (i.) how to acquire a reliable estimate of the segmentation model performance as quickly as possible; and (ii.) how to improve the training process of the segmentation architecture through over-parameterisation, obsolete during inference.

3.1. Problem Formulation

We consider dense prediction task T , for which we have multiple training tuples $\{(X_i, y_i)\}$, where both X_i and y_i are 3-dimensional tensors with equal spatial and arbitrary third dimensions. In this work, X_i is a 3-channel RGB image, while y_i is a C -channel one-hot segmentation mask with C being equal to the number of classes, which corresponds to semantic image segmentation. Furthermore, we rely on a mapping $f : X \rightarrow y$ with parameters θ , that is represented by a fully convolutional neural network. We assume that the network f can further be decomposed into two parts: e - representing encoder, and d - for decoder. We initialise encoder e with weights from a pre-trained classification network consisting of multiple down-sampling operations that reduce the spatial dimensions of the input. The decoder part, on the other hand, has access to several outputs of encoder with varying spatial and channel dimensions. The search goal is to choose which feature maps to use and what operations to apply on them. We next describe the decoder search space in full detail.

3.1.1 Search Space

We restrict our attention to the decoder part, as it is currently infeasible to perform a full segmentation network search from scratch. As mentioned above, decoder has access to multiple layers from the pre-trained encoder with varying dimensions. We rely on a recurrent neural network, controller, to sequentially produce pairs of indices of which layers to use, and what operations to apply on them. In particular, this sequence of operations is combined to form a cell. The same cell but with different weights is applied on each of the sampled pair of indices, and the outputs of two cells are summed up. The aggregated location can further be sampled by the controller. Whereas the cell design is only sampled once per each architecture, the number of location samples is controlled by an additional hyper-parameter, which is set to 3 in our experiments. All existing non-sampled aggregated locations are concatenated, before being fed into a single 1×1 convolution to reduce the number of channels followed by the final classifier layer.

Each cell takes a single input with the controller deciding which operation to use on that input. The controller then proceeds by sampling with replacement two locations out of two, i.e., of input and the result of the first operation on input, and two corresponding operations. The results of each operation are summed up, and all three locations (from each operation and their aggregation) together with the initial two can be sampled on the next step. The number of times the locations are being sampled inside the cell is controlled by another hyper-parameter, which we also set to 3 in our experiments in order to keep the number of all possible architectures to a feasible amount. All existing non-sampled aggregated locations inside the cell are summed up, and used as the cell output.

Based on existing research in semantic segmentation, we consider 11 operations:

- conv 1×1 ,
- conv 3×3 ,
- separable conv 3×3 ,
- separable conv 5×5 ,
- global average pooling followed by upsampling and conv 1×1 ,
- conv 3×3 with dilation rate 3,
- conv 3×3 with dilation rate 12,
- separable conv 3×3 with dilation rate 3,
- separable conv 5×5 with dilation rate 6,
- skip-connection,
- zero-operation that effectively nullifies the path.

An example of search layout is depicted on Fig. 1.

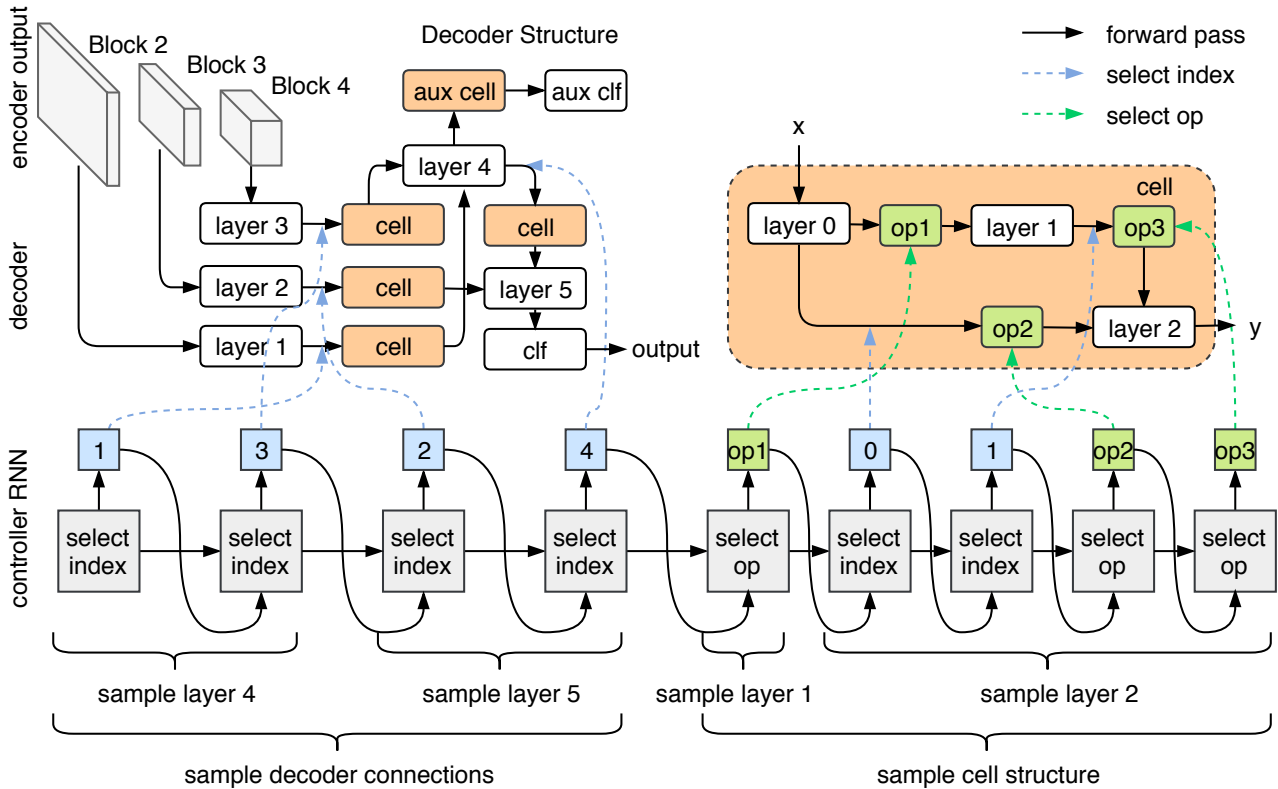


Figure 1 – Encoder-decoder auxiliary search layout. Controller RNN (*bottom*) first generates connections between encoder and decoder (*top left*), and then samples locations and operations to use inside the cell (*top right*). All the cells (including auxiliary cell) share the emitted design.

3.2. Search Strategy

We divide the training set into two disjoint sets - meta-train and meta-val. The meta-train subset is used to train the sampled architecture on the given task (i.e., semantic segmentation), whereas meta-val, on the other hand, is used to evaluate the trained architecture and provide the controller with a scalar, oftentimes called *reward* in the reinforcement learning literature. Given the sampled sequence, its logarithmic probabilities and the reward signal, the controller is optimised via proximal policy optimisation (PPO) [34]. Hence, there are two training processes present: inner - optimisation of the sampled architecture on the given task, and outer - optimisation of the controller. We next concentrate on the inner loop.

3.2.1 Progressive Stages

We divide the inner training process into two stages. During the first stage, the encoder weights are fixed and its outputs are pre-computed, while only decoder is being trained. This leads to a quick adaptation of the decoder weights and a reasonable estimate of the performance of the sampled architecture. Then we exploit a simple heuristic to decide

whether to continue training the sampled architecture for the second stage, or not. Concretely, the current reward value is being compared with the running mean of rewards seen so far, and if it is higher, we continue training. Otherwise, with probability $1 - p$ we terminate the training process. The probability p is annealed throughout our search (starting from 0.9).

The motivation behind this is straightforward: the results of the first stage, while noisy, can still provide a reasonable estimate of the potential of the sampled architecture. To the very least, they would present a reliable signal that the sampled architecture is non-promising, while spending only few seconds on it.

3.2.2 Fast Training via Knowledge Distillation and Weights' Averaging

Semantic segmentation models are notable for requiring lots of iterations to converge. Partially, this is addressed by initialising the encoder part from a pre-trained classification network. Unfortunately, no such thing exists for decoder.

Fortunately, though, we can explore several alternatives that provide faster convergence. Besides tailoring our optimisation hyper-parameters, we rely on two more tricks:

firstly, we keep track of the running average of the parameters during each stage and apply them before the final validation [29]. Secondly, we append an additional l_2 -loss term between the logits of the current architecture and a pre-trained teacher network. We can either pre-compute the teacher’s outputs beforehand, or acquire them on-the-fly in case the teacher’s computations are negligible.

The combination of both of these approaches allows us to receive a very reliable estimate of the performance of the semantic segmentation model as quickly as possible without a significant overhead.

3.2.3 Intermediate Supervision via Auxiliary Cells

We further look for ways of easing optimisation during the inner training stage, as well as during the general training of semantic segmentation models. This may not only improve the convergence speed, but also the convergence optimality. Thus, still aligning with the goal of having a compact but accurate model during the inference time, we explicitly aim to find ways of performing steps that are beneficial during training and obsolete during evaluation.

One approach that we consider here is to append an auxiliary cell after each summation between pairs of main cells - the auxiliary cell has identical to the main cell design and can either be conditioned to output ground truth directly, or to mimic the teacher’s network predictions (or the combination of the above two). At the same time, it does not influence the output of the main classifier either during the training or testing and merely provides better gradients for the rest of the network. In the end, the reward per the sampled architecture will still be decided by the output of the main classifier. For simplicity, we only apply the segmentation loss on all auxiliary outputs.

The notion of intermediate supervision is not novel in neural networks, but to the best of our knowledge, prior works have merely been relying on a simple auxiliary classifier, and we are the first to tie up the design of decoder with the design of the auxiliary cell. We demonstrate the quantitative benefits of doing so in our ablation studies (Sect. 4.2).

Furthermore, our motivation behind searching for cells that may also serve as intermediate supervisors stems from ever-growing empirical (and theoretical under certain assumptions) evidence that deep networks benefit from over-parameterisation during training [8, 37]. Oftentimes such an over-parameterisation can be exploited by the means of compression algorithms - *e.g.*, pruning [11]. While auxiliary cells provide an implicit notion of over-parameterisation, we could have explicitly increased the number of channels and then resorted to pruning, but pruning methods tend to result in unstructured networks that carry almost no practical benefits in terms of the runtime speed. Our solution in this sense simply permits omitting

unused layers during inference.

4. Experiments

We conduct extensive experiments on PASCAL VOC which is an established semantic segmentation benchmark that comprises 20 semantic classes and provides 1464 training images [9]. For the search process, we extend those to more than 10000 by exploiting annotations from BSD [12]. As commonly done, during search, we keep 10% of those images for validation of the sampled architectures that provides the controller with the reward signal. For the first stage, we pre-compute the encoder outputs on 4000 images and store them for faster processing.

The controller is a two-layer recurrent LSTM [14] neural network with 100 hidden units. All the units are randomly initialised from uniform distribution. We use PPO [34] for optimisation with the learning rate of 0.0001.

The encoder part of our network is MobileNet-v2 [32], pretrained on MS COCO [20] for semantic segmentation using the Light-Weight RefineNet decoder [26]. We omit the last layers and consider four outputs from layers 2, 3, 6, 8 as inputs to decoder. Decoder weights are randomly initialised using the Xavier scheme [10]. To perform knowledge distillation, we use Light-Weight RefineNet-152 [26], and apply l_2 -loss with the coefficient of 0.3. The knowledge distillation outputs are pre-computed for the first stage and omitted during the second one in the interests of time. Polyak averaging is applied with the decay rates of 0.9 and 0.99, correspondingly. Batch normalisation statistics are updated during both stages.

All our experiments are being conducted on two 1080Ti GPU cards, with the search process being terminated after 4 days. All runtime measurements are carried out on a single 1080Ti card, or on JetsonTX2, if mentioned otherwise. In particular, we perform the forward pass 100 times and report the mean result together with standard deviation.

4.1. Search Results

For the inner training of the sampled architectures, we devise a fast and stable training strategy: we exploit the Adam learning rule [16] for the decoder part of the network, and SGD with momentum - for encoder. In particular, we use learning rates of $3e - 3$ and $1e - 3$, respectively. We pre-train each sampled architecture for 5 epochs on the first stage, and for 1 on the second (in case the stopping criterion is not triggered). As the reward signal, we consider the geometric mean of three quantities: namely,

- i.) mean intersection-over-union (IoU), or Jaccard Index [9], primarily used across semantic segmentation benchmarks;
- ii.) frequency-weighted IoU, that scales each class IoU by the number of pixels present in that class, and

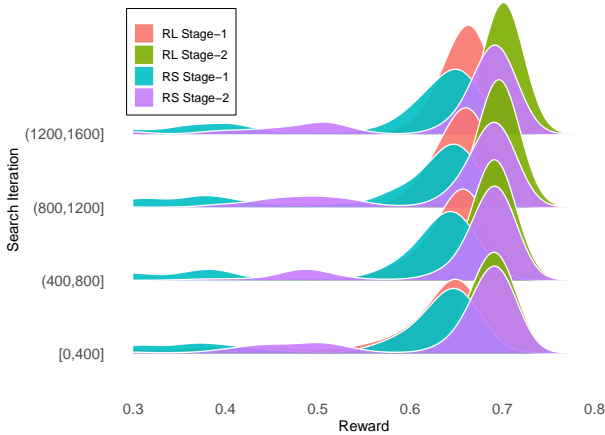


Figure 2 – Distribution of rewards per each training stage for reinforcement learning (RL) and random search (RS) strategies.

iii.) mean-pixel accuracy, that averages the number of correct pixels per each class. When computing, we do not include background class as it tends to skew the results due to a large number of pixels belonging to background. As mentioned above, we keep the running mean of rewards after the first stage to decide whether to continue training a sampled architecture.

We visualise the reward progress during both stages on Figure 2. As evident from it, the quality of the emitted architectures grows with time - it is even possible that more iterations would lead to better results, although we do not explore that to save the time spent. On the other hand, while random search is potent of occasionally sampling decent architectures, it does only arrive at a fraction of them in comparison to the RL-based controller.

Moreover, we evaluate the impact of the inclusion of Polyak averaging, auxiliary cells and knowledge distillation on each training stage. To this end, we randomly sample and train 140 architectures. We visualise the distributions

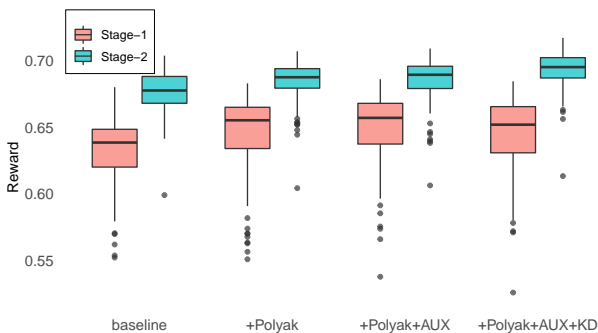


Figure 3 – Distribution of rewards during each training stage of the search process across setups with Polyak averaging (Polyak), intermediate supervision through auxiliary cells (AUX) and knowledge distillation (KD).

of rewards on Fig. 3. All the tested settings significantly outperform baseline on both stages, and the highest rewards on the second stage are attained when using all of the components above.

4.2. Effect of Intermediate Supervision via Auxiliary Cells

After the search process is finished, we sample 10 architectures from the controller and proceed by carrying out additional ablation studies aimed to estimate the benefit of the proposed auxiliary scheme in case the architectures are allowed to train for longer.

In particular, we train each architecture for 10 epochs on BSD together with PASCAL VOC and 20 epochs on PASCAL VOC only. For simplicity, we omit Polyak averaging and knowledge distillation. Four distinct setups are being tested: concretely, we estimate whether intermediate supervision helps at all, and whether concatenation or summation is better before the final classifier is applied.

The results of these ablation studies are given on Fig. 4. Auxiliary supervised architectures achieve highest mean IoU, and, in particular, concatenation of intermediate outputs leads to best results for 8 out of 10 architectures.

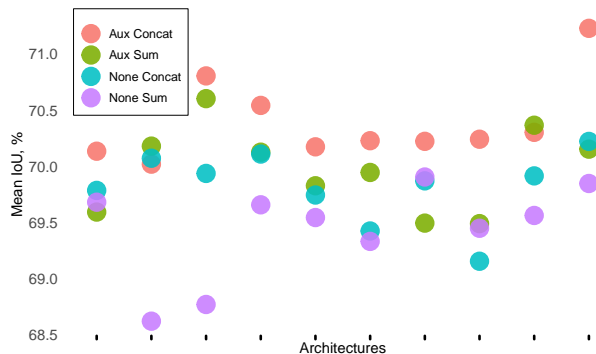


Figure 4 – Ablation studies on the necessity of intermediate supervision (Aux), and the aggregation operation to be used before final classification (Sum or Concat). Each tick on the x-axis corresponds to a different architecture.

4.3. Full Training Results

Finally, we choose 3 best performing architectures from Sect. 4.2 and train each on the full training set, augmented with annotations from MS COCO [20]. The training setup is analogous to the aforementioned one with the first stage being trained for 20 epochs (on COCO+BSD+VOC), the second stage - for 20 (BSD+VOC), and the last one - for 30 (VOC only). Halfway through the first stage we freeze the batch norm statistics and divide learning rate in half. Correspondingly, after each stage the learning rate is halved again. We exploit intermediate supervision via auxiliary cell with coefficients of 0.3, 0.25, 0.2, 0.15 across the

stages.

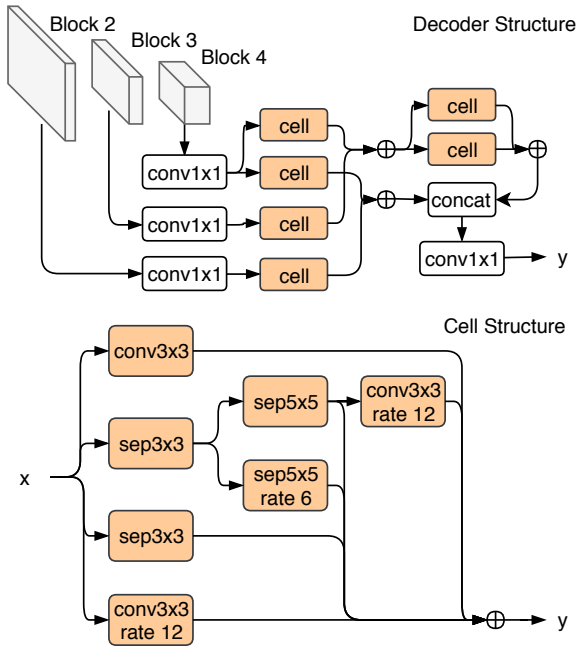


Figure 5 – Automatically discovered decoder architecture (*arch0*). We visualise the connectivity structure between encoder and decoder (*top*), and the cell design (*bottom*). \oplus represents an element-wise summation operation applied to each branch scaled to the highest spatial resolution among them (via bilinear interpolation).

Quantitative results are given in Table 1 and few qualitative examples are on Fig. 6. The architectures discovered by our method achieve competitive performance in comparison to state-of-the-art compact models and even do so with a significantly lower number of floating point operations and parameters. At the same time, the found architectures can be run in real-time both on a generic GPU card and JetsonTX2.

We visualise the structure of the highest performing architecture (*arch0*) on Fig. 5. Having multiple branches encoding information of different scales, it resembles several prominent blocks in semantic segmentation, notably the ASPP module [7]. Importantly, the cell found by our method differs in the way the receptive field size is controlled. Whereas ASPP solely relies on various dilation rates, here several kernel sizes arranged in a cascaded manner allow much more flexibility. Furthermore, this design is more computationally efficient and has better expressiveness as intermediate features can be easily re-used.

4.4. Transferrability to other Dense Output Tasks

4.4.1 Pose Estimation

We further apply the best found architecture on the task of pose estimation. In particular, the MPII [1] and MS COCO Keypoint [20] datasets are used as our benchmark. MPII

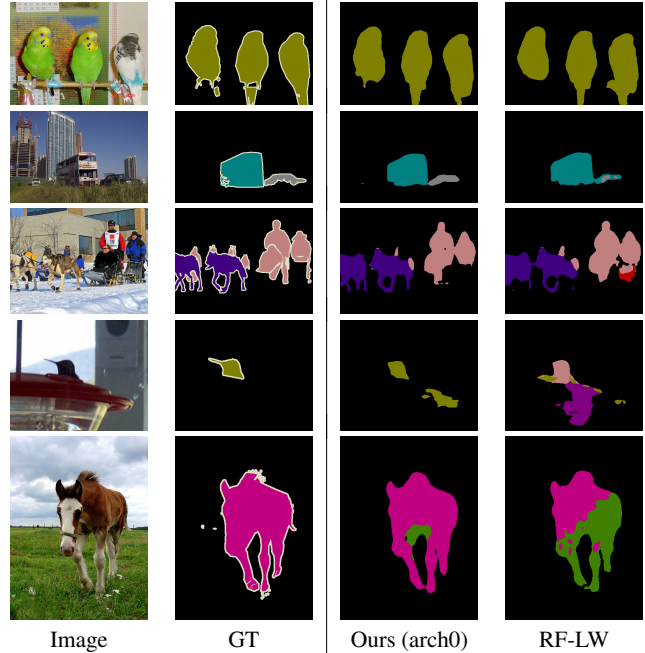


Figure 6 – Inference results of our model (*arch0*) on validation set of PASCAL VOC and Light-Weight-RefineNet (*RF-LW*). Both models rely on MobileNet-v2 as the encoder.

includes 25K images containing 40K people with 16 annotated body joints. The evaluation measure is PCKh [33] with thresholds of 0.5 and 0.1. The COCO dataset comprises 200K images of 250K people with 17 body joints. Based on object keypoint similarity (OKS)¹, we report average precision (AP) and average recall (AR) over 10 different OKS thresholds.

Our quantitative results are in Table 2 and few qualitative examples are on Fig. 7. We follow the training protocol of Xiao *et al.* [42] and do not tune our architecture. As can be seen from the results, our discovered architecture achieves competitive performance even in comparison to a more powerful ResNet-50-based model.

4.4.2 Depth Estimation

Finally, we train the best found architecture on NYUDv2 [35] for the depth estimation task. Following previous work [25], we only use 25K training images with depth annotations collected with the Kinect sensor. We report validation results on 654 images in Table 3 and visualise few examples on Fig. 8. Among other compact real-time networks, we achieve best results across all the metrics without any additional tricks. Note also that the work in [25] trained the depth model jointly with semantic segmentation, thus using extra information.

¹<http://cocodataset.org/#keypoints-eval>

Model	Val mIoU, %	FLOPs, B	Params, M	Output Res	Runtime, ms (JetsonTX2/1080Ti)	
DeepLab-v3-ASPP [32]	75.7	5.8	4.5	32×32	69.67±0.53	8.09±0.53
DeepLab-v3 [32]	75.9	8.73	2.1	64×64	122.07±0.58	11.35±0.43
RefineNet-LW [26]	76.2	9.3	3.3	128×128	144.85±0.49	12.00±0.26
Ours (arch0)	76.1	2.95	2.8	64×64	67.57±0.54	11.04±0.23
Ours (arch1)	75.2	3.42	2.8	64×64	77.16±0.34	10.25±0.22
Ours (arch2)	75.6	3.47	2.9	64×64	64.60±0.33	8.86±0.26

Table 1 – Results on validation set of PASCAL VOC after full training on COCO+SBD+VOC. All networks share the same backbone - MobileNet-v2. FLOPs and runtime are being measured on 512×512 inputs. For DeepLab-v3 we use official models provided by the authors.



Figure 7 – Inference results of our model (*arch0*) on validation set of MPII, along with that of DeepLab-v3+-MobileNet-v2 and ResNet-50 [42].

Model	MPII		COCO		Params, M
	Mean@0.5	Mean@0.1	AP	AR	
DeepLab-v3+ [7]	86.6	31.7	0.668	0.700	5.8
ResNet-50 [42]	88.5	33.9	0.704	0.763	34.0
Ours (arch0)	86.6	31.3	0.659	0.694	2.8

Table 2 – Comparisons on MPII validation and COCO val2017. Flip test is used. For COCO, the same detector as in [42] is used for all models. DeepLab-v3+ is our re-implementation based on the official code.

	Ours	CReaM <i>et al.</i> [38]	RF-LW [25]
RMSE (lin)	0.552	0.687	0.565
RMSE (log)	0.198	0.251	0.205
abs rel	0.147	0.190	0.149
sqr rel	0.102	–	0.105
$\delta < 1.25$	0.807	0.704	0.790
$\delta < 1.25^2$	0.959	0.917	0.955
$\delta < 1.25^3$	0.990	0.977	0.990
Parameters, M	2.8	1.5	3.0

Table 3 – Quantitative results on the validation set of NYUDv2. For RMSE, abs rel and sqr rel lower values are better, whereas for accuracy (δ) higher values are better.

5. Discussion and Conclusions

There is little doubt that manual design of neural architectures is a tedious and difficult task to handle. It is even more complicated to come up with a design of compact and high-performing architecture on challenging dense predic-

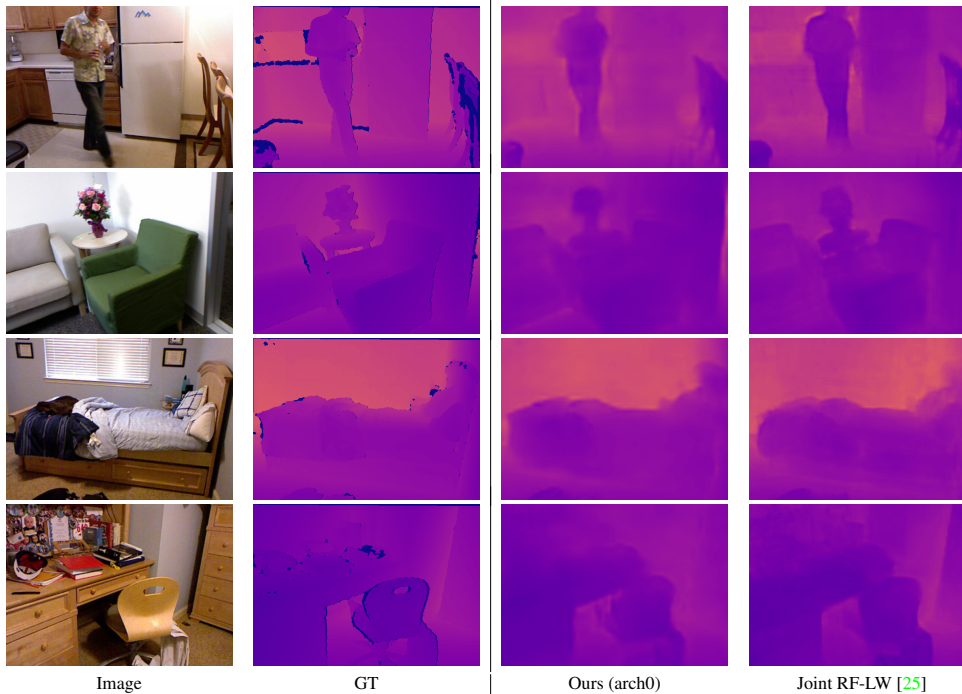


Figure 8 – Our depth estimation qualitative results on NYUDv2, along with that of Joint Light-Weight RefineNet [25]. Dark-blue pixels in ground truth are pixels with missing depth measurements.

tion problems, such as semantic segmentation. In this work, we showcased a simple and reliable approach of searching for fully convolutional architectures within a reasonable amount of time and computational resources. Our method is based around over-parameterisation of small networks that allows them to converge to better solutions. We achieved competitive performance to manually designed state-of-the-art compact architectures, while searching only for 4 days on 2 GPU cards.

Our goals are to explore alternative ways of over-parameterisation, search space description and transferability of our search methodology to other dense per-pixel tasks.

Acknowledgements

VN, CS, IR’s participation in this work were in part supported by ARC Centre of Excellence for Robotic Vision. CS was also supported by the GeoVision CRC Project. Correspondence should be addressed to CS.

References

[1] M. Andriluka, L. Pishchulin, P. Gehler, and B. Schiele. 2d human pose estimation: New benchmark and state of the art analysis. In *Proc. IEEE Conf. Comp. Vis. Patt. Recogn.*, 2014. 7

[2] P. J. Angeline, G. M. Saunders, and J. B. Pollack. An evolu-

tionary algorithm that constructs recurrent neural networks. *IEEE Trans. Neural Networks*, 1994. 1, 2

[3] B. Baker, O. Gupta, N. Naik, and R. Raskar. Designing neural network architectures using reinforcement learning. *Proc. Int. Conf. Learn. Representations*, 2017. 1, 2

[4] J. Bergstra, D. Yamins, and D. D. Cox. Making a science of model search: Hyperparameter optimization in hundreds of dimensions for vision architectures. In *Proc. Int. Conf. Mach. Learn.*, 2013. 2

[5] L. Chen, M. D. Collins, Y. Zhu, G. Papandreou, B. Zoph, F. Schroff, H. Adam, and J. Shlens. Searching for efficient multi-scale architectures for dense image prediction. *Proc. Advances in Neural Inf. Process. Syst.*, 2018. 3

[6] L. Chen, G. Papandreou, I. Kokkinos, K. Murphy, and A. L. Yuille. Deeplab: Semantic image segmentation with deep convolutional nets, atrous convolution, and fully connected crfs. *IEEE Trans. Pattern Anal. Mach. Intell.*, 2018. 2

[7] L. Chen, Y. Zhu, G. Papandreou, F. Schroff, and H. Adam. Encoder-decoder with atrous separable convolution for semantic image segmentation. In *Proc. Eur. Conf. Comp. Vis.*, 2018. 2, 7, 8

[8] S. Du and J. Lee. On the power of over-parametrization in neural networks with quadratic activation. In *Proc. Int. Conf. Mach. Learn.*, 2018. 2, 5

[9] M. Everingham, L. J. V. Gool, C. K. I. Williams, J. M. Winn, and A. Zisserman. The pascal visual object classes (VOC) challenge. *Int. J. Comput. Vision*, 2010. 5

[10] X. Glorot and Y. Bengio. Understanding the difficulty of training deep feedforward neural networks. In *Proc. Int. Conf. Artificial Intell. & Stat.*, 2010. 5

- [11] S. Han, X. Liu, H. Mao, J. Pu, A. Pedram, M. Horowitz, and B. Dally. Deep compression and EIE: efficient inference engine on compressed deep neural network. In *IEEE Hot Chips Symposium*, 2016. 5
- [12] B. Hariharan, P. Arbelaez, L. D. Bourdev, S. Maji, and J. Malik. Semantic contours from inverse detectors. In *Proc. IEEE Int. Conf. Comp. Vis.*, 2011. 5
- [13] G. E. Hinton, O. Vinyals, and J. Dean. Distilling the knowledge in a neural network. *Proc. Advances in Neural Inf. Process. Syst.*, 2014. 2, 3
- [14] S. Hochreiter and J. Schmidhuber. Long short-term memory. *Neural Computation*, 1997. 5
- [15] K. Kandasamy, W. Neiswanger, J. Schneider, B. Póczos, and E. Xing. Neural architecture search with bayesian optimisation and optimal transport. *arXiv: Comp. Res. Repository*, 2018. 2
- [16] D. P. Kingma and J. Ba. Adam: A method for stochastic optimization. *arXiv: Comp. Res. Repository*, abs/1412.6980, 2014. 5
- [17] Z. Li and D. Hoiem. Learning without forgetting. In *Proc. Eur. Conf. Comp. Vis.*, 2016. 3
- [18] G. Lin, A. Milan, C. Shen, and I. D. Reid. RefineNet: Multi-path refinement networks for high-resolution semantic segmentation. In *Proc. IEEE Conf. Comp. Vis. Patt. Recogn.*, 2017. 2
- [19] G. Lin, C. Shen, I. D. Reid, and A. van den Hengel. Efficient piecewise training of deep structured models for semantic segmentation. *Proc. IEEE Conf. Comp. Vis. Patt. Recogn.*, pages 3194–3203, 2016. 2
- [20] T. Lin, M. Maire, S. J. Belongie, J. Hays, P. Perona, D. Ramanan, P. Dollár, and C. L. Zitnick. Microsoft COCO: common objects in context. In *Proc. Eur. Conf. Comp. Vis.*, 2014. 5, 6, 7
- [21] C. Liu, B. Zoph, M. Neumann, J. Shlens, W. Hua, L. Li, L. Fei-Fei, A. L. Yuille, J. Huang, and K. Murphy. Progressive neural architecture search. In *Proc. Eur. Conf. Comp. Vis.*, 2018. 1, 2
- [22] H. Liu, K. Simonyan, O. Vinyals, C. Fernando, and K. Kavukcuoglu. Hierarchical representations for efficient architecture search. *Proc. Int. Conf. Learn. Representations*, 2018. 2
- [23] J. Long, E. Shelhamer, and T. Darrell. Fully convolutional networks for semantic segmentation. In *Proc. IEEE Conf. Comp. Vis. Patt. Recogn.*, 2015. 2
- [24] R. Luo, F. Tian, T. Qin, and T. Liu. Neural architecture optimization. *Proc. Advances in Neural Inf. Process. Syst.*, 2018. 2
- [25] V. Nekrasov, T. Dharmasiri, A. Spek, T. Drummond, C. Shen, and I. D. Reid. Real-time joint semantic segmentation and depth estimation using asymmetric annotations. *arXiv: Comp. Res. Repository*, abs/1809.04766, 2018. 7, 8, 9
- [26] V. Nekrasov, C. Shen, and I. D. Reid. Light-weight refinenet for real-time semantic segmentation. In *Proc. British Machine Vis. Conf.*, 2018. 5, 8
- [27] H. Noh, S. Hong, and B. Han. Learning deconvolution network for semantic segmentation. In *Proc. IEEE Int. Conf. Comp. Vis.*, 2015. 2
- [28] H. Pham, M. Y. Guan, B. Zoph, Q. V. Le, and J. Dean. Efficient neural architecture search via parameter sharing. In *Proc. Int. Conf. Mach. Learn.*, 2018. 1, 2
- [29] B. T. Polyak and A. B. Juditsky. Acceleration of stochastic approximation by averaging. *SIAM Journal on Control and Optimization*, 1992. 2, 5
- [30] E. Real, S. Moore, A. Selle, S. Saxena, Y. L. Suematsu, J. Tan, Q. V. Le, and A. Kurakin. Large-scale evolution of image classifiers. In *Proc. Int. Conf. Mach. Learn.*, 2017. 2
- [31] A. A. Rusu, S. G. Colmenarejo, Ç. Gülçehre, G. Desjardins, J. Kirkpatrick, R. Pascanu, V. Mnih, K. Kavukcuoglu, and R. Hadsell. Policy distillation. *Proc. Int. Conf. Learn. Representations*, 2016. 3
- [32] M. Sandler, A. G. Howard, M. Zhu, A. Zhmoginov, and L. Chen. Inverted residuals and linear bottlenecks: Mobile networks for classification, detection and segmentation. *Proc. IEEE Conf. Comp. Vis. Patt. Recogn.*, 2018. 5, 8
- [33] B. Sapp and B. Taskar. MODEC: multimodal decomposable models for human pose estimation. In *Proc. IEEE Conf. Comp. Vis. Patt. Recogn.*, pages 3674–3681, 2013. 7
- [34] J. Schulman, F. Wolski, P. Dhariwal, A. Radford, and O. Klimov. Proximal policy optimization algorithms. *arXiv: Comp. Res. Repository*, 2017. 4, 5
- [35] N. Silberman, D. Hoiem, P. Kohli, and R. Fergus. Indoor segmentation and support inference from RGBD images. In *Proc. Eur. Conf. Comp. Vis.*, 2012. 7
- [36] J. Snoek, H. Larochelle, and R. P. Adams. Practical bayesian optimization of machine learning algorithms. In *Proc. Advances in Neural Inf. Process. Syst.*, 2012. 2
- [37] M. Soltanolkotabi, A. Javanmard, and J. D. Lee. Theoretical insights into the optimization landscape of over-parameterized shallow neural networks. *IEEE Transactions on Information Theory*, 2018. 2, 5
- [38] A. Spek, T. Dharmasiri, and T. Drummond. CReaM: Condensed real-time models for depth prediction using convolutional neural networks. *Proc. IEEE/RSJ Int. Conf. Intelligent Robots & Systems*, 2018. 8
- [39] K. O. Stanley, D. B. D’Ambrosio, and J. Gauci. A hypercube-based encoding for evolving large-scale neural networks. *Artificial Life*, 2009. 2
- [40] K. O. Stanley and R. Miikkulainen. Evolving neural network through augmenting topologies. *Evolutionary Computation*, 2002. 2
- [41] K. Swersky, D. Duvenaud, J. Snoek, F. Hutter, and M. A. Osborne. Raiders of the lost architecture: Kernels for bayesian optimization in conditional parameter spaces. *arXiv: Comp. Res. Repository*, 2014. 2
- [42] B. Xiao, H. Wu, and Y. Wei. Simple baselines for human pose estimation and tracking. In *Proc. Eur. Conf. Comp. Vis.*, 2018. 7, 8
- [43] F. Yu, V. Koltun, and T. A. Funkhouser. Dilated residual networks. In *Proc. IEEE Conf. Comp. Vis. Patt. Recogn.*, 2017. 2
- [44] A. R. Zamir, A. Sax, W. B. Shen, L. J. Guibas, J. Malik, and S. Savarese. Taskonomy: Disentangling task transfer learning. *Proc. IEEE Conf. Comp. Vis. Patt. Recogn.*, 2018. 3
- [45] H. Zhao, J. Shi, X. Qi, X. Wang, and J. Jia. Pyramid scene parsing network. In *Proc. IEEE Conf. Comp. Vis. Patt. Recogn.*, 2017. 2
- [46] B. Zoph and Q. V. Le. Neural architecture search with rein-

forcement learning. *Proc. Int. Conf. Learn. Representations*, 2017. [1](#), [2](#)

- [47] B. Zoph, V. Vasudevan, J. Shlens, and Q. V. Le. Learning transferable architectures for scalable image recognition. *Proc. IEEE Conf. Comp. Vis. Patt. Recogn.*, 2018. [1](#), [2](#)